Structural response of composite plates equipped with piezoelectric actuators

Amâncio Fernandes, J. Pouget

Structural response of composite plates equipped with piezoelectric actuators

A. Fernandes [a,*] and J. Pouget [b]

[a] *Laboratoire de Modélisation en Mécanique (UMR 7607), Université Pierre et Marie Curie, Case 162, 4 Place Jussieu 75252 Paris Cedex 05, France*

[b] *Laboratoire d'Etudes Mécaniques des Assemblages (FRE 2481), Université de Versailles/Saint-Quentin-en-Yvelines, Bâtiment Descartes, 45 Ave des Etats-Unis, 78035 Versailles Cedex, France*

Abstract

We propose the modelling of piezoelectric elements perfectly bonded on an elastic structure. The study aims at predicting the static and dynamic (vibration) electromechanical responses of the structure. The model is mostly based on the kinematic assumption of the Love-Kirchhoff thin plate theory including shear function with a quadratic variation of the electric potential along the thickness direction of the piezoelectric parts. A variational formulation of piezoelectricity leads to the equations of motion for an elastic plate equipped with piezoelectric elements. An important feature of the present investigation is that the stiffness and inertial contributions of the piezoelectric patch is not neglected. Moreover, the numerical simulations demonstrate the influence of the actuator position on the global and local responses of the elastic plate for two situations (i) bilayer and (ii) sandwich configurations. A number of benchmark tests are considered in order to characterize the plate deformation when applying an electric potential to the piezoelectric patch faces. Plate vibration problem is also presented and the frequencies for the axial and flexural modes are obtained. The spectra of vibration for the plate with a time-dependent electric potential are computed.

Key words: Piezoelectric patch, actuators, plate vibration, closed-form solution.

1 Introduction

Piezoelectric materials, and especially piezoelectric composites such as multilayered plates including active piezoelectric layers are excellent candidates for de-

* Corresponding author. Tel.:+33144278713; Fax: +33144275259
Email address: fernande@lmm.jussieu.fr (A. Fernandes).

signing adaptive devices for shape and vibration control of elastic structures. Such devices and piezoelectric composites are of great technological interest in structural engineering with applications to noise reduction or shape control of large flexible structures (shape control of space antennas or telescopes) [1].

Most modellings of piezoelectric actuators or composites consider laminated structures made of continuous piezoelectric layers. The models are mainly based on thin plate theory including some refinements and possible layerwise approach [2,3]. Nevertheless, very few models of piezoelectric elements or patches bonded on elastic structures have been examined and quoted in literature [4,5,6]. The simplest approaches to elastic structures (beam, plate, etc.) equipped with piezoelectric elements consider effective forces and moments induced by piezoelectric elements on the host structure [7]. In such approaches the driving forces and moments are generated by the electric potential applied to the piezoelectric element, however, the sensor function of the piezoelectric element is usually not accounted for. A first order shear deformation theory has been considered to describe the electromechanical state of the element bonded on an elastic structure (beam or plate). The extensional-flexural motion of the beam is then governed by a set of coupled equations for the elongational displacement, deflection and electric potential or electric charge. However, analytical results are based on either Euler-Bernoulli beam theory or Timoshenko beam modelling [7]. In most analysis it is assumed that the stiffness and inertial contribution of the piezoelectric actuators are neglected in comparison to those of the host elastic structure [4]. Such an assumption leads to inaccurate estimate of the electromechanical responses of the structure. Especially, the prediction of the frequencies of axial and flexural modes of the composite structure requires a more accurate approach.

The present work concerns the modelling of a composite structure made of a piezoelectric element perfectly attached to an elastic thin plate. Moreover, the model considers two kinds of kinematical hypotheses either for the elastic plate or for the piezoelectric actuator. For the elastic plate a refined description of the elastic displacement is considered, it is based on the Love-Kirchhoff elastic thin plate theory including a shear function [8,9]. For the piezoelectric element the kinematical hypothesis of the Love-Kirchhoff plate theory is merely adopted. The electric potential is supposed to have a quadratic variation through the piezoelectric layer thickness [8,9]. In the proposed formulation there are no simplifying hypotheses on the stiffness and inertial contribution of the piezoelectric elements. In fact, the piezoelectric part introduces material and geometrical discontinuities which lead to some mathematical difficulties. In spide of these drawbacks, a closed-form solution to the equation of motion can be obtained by using Fourier analysis for an elastic plate simply supported under cylindrical bending and the solution for static and dynamic processes are computed.

2 Variational formulation and governing equations

Let us define the following affine spaces

$$\mathcal{V}_u = \{(\mathbf{u}, \mathbf{S}) \ : \ \mathbf{u} = \mathbf{u}_0 \quad \text{on } \partial\Omega_u \quad \text{and} \quad S_{ij} = u_{(i,j)} \quad \text{on } \Omega\} \ , \tag{1a}$$
$$\mathcal{V}_\phi = \{(\phi, \mathbf{E}) \ : \ \phi = \phi_0 \quad \text{on } \partial\Omega_\phi \quad \text{and} \quad E_i = -\phi_{,i} \quad \text{on } \Omega\} \ , \tag{1b}$$

where $\mathcal{V}_u$ is the space of kinematically admissible displacements and strain tensors and $\mathcal{V}_\phi$ is the space of admissible electric potential and electric field. In Eqs (1) $\mathbf{u}$ and $\mathbf{S}$ are respectively the displacement and the linear part of the strain tensor. The scalar variable ϕ is the electric potential. In the framework of the quasi-electrostatic approximation, the electric field $\mathbf{E}$ derives from an electric potential $E_i = -\phi_{,i}$. We consider the functional extended to piezoelectric materials written as follows [10]

$$\mathcal{F}[(\mathbf{u}, \mathbf{S}) \, , (\phi, \mathbf{E})] = \int_\Omega \left(-H \left(\mathbf{S}, \mathbf{E} \right) + \overline{\mathbf{b}} \cdot \mathbf{u} \right) dv + \int_{\partial\Omega_T} \mathbf{T} \cdot \mathbf{u} \, da + \int_{\partial\Omega_q} q_0 \phi \, da \ , \tag{2}$$

defined over the space $\mathcal{V} = \mathcal{V}_u \times \mathcal{V}_\phi$. In the functional $\mathcal{F}$, $H \left(\mathbf{S}, \mathbf{E} \right)$ is the electric enthalpy density functional given by [10]

$$H \left(\mathbf{S}, \mathbf{E} \right) = \frac{1}{2} \sigma_{ij} S_{ij} - \frac{1}{2} D_i E_i \ , \tag{3}$$

where σ is the stress tensor and $\mathbf{D}$ is the electric displacement or induction vector. In Eq. (2), $\overline{\mathbf{b}}$ is an external force per unit volume applied on Ω (including eventually inertial forces $\overline{b}_i = f_i - \rho \ddot{u}_i$). In the second part of Eq. (2), $\mathbf{T}$ is the surface density of traction forces imposed on $\partial\Omega_T$ and, in the third part, q_0 is the surface density of electric charges applied on $\partial\Omega_q$.
Under suitable regularity conditions, the balance equations for piezoelectric body are found by imposing vanishing first variations of the functional Eq. (2) with respect to $\mathbf{u}$ and ϕ. They read as

$$\sigma_{ij,j} + \overline{b}_i = 0 \ , \qquad D_{i,i} = 0 \ . \tag{4}$$

The boundary conditions on $\partial\Omega$ are also obtained from the variation of the functional Eq. (2). They are $\sigma_{ij} n_j = T_i$ on $\partial\Omega_T$ and $D_i n_i = q_0$ on $\partial\Omega_q$ for the natural boundary conditions and $\mathbf{u} = \mathbf{u_0}$ on $\partial\Omega_u$ and $\phi = \phi_0$ on $\partial\Omega_\phi$ for the essential boundary conditions ($\partial\Omega = \partial\Omega_T \cup \partial\Omega_u = \partial\Omega_q \cup \partial\Omega_\phi$ with $\partial\Omega_T \cap \partial\Omega_u = \partial\Omega_q \cap \partial\Omega_\phi = \varnothing$). The constitutive equations are given in the $\mathbf{S} - \mathbf{E}$ form through

the electric enthalpy functional Eq. (3) and they are given by

$$\sigma_{ij} = \frac{\partial H}{\partial S_{ij}} = C^E_{ijpq} S_{pq} - e_{kij} E_k \ , \tag{5a}$$

$$D_i = -\frac{\partial H}{\partial E_i} = e_{ipq} S_{pq} + \varepsilon^S_{ij} E_j \ , \tag{5b}$$

where, $\mathbf{C}^E$ is the tensor of elasticity coefficients for null electric field, $\mathbf{e}$ is the piezoelectric coupling third-order tensor and ε^S is the second-order tensor of electric permittivity coefficients for null strain. The variational formulation given in Eqs (2) and (3) and the set of Eqs (4) and (5) are the essential starting point of the modelling proposed in the forthcoming sections.

3 Field approximation

Let us consider an elastic plate equipped with a piezoelectric element as depicted in Fig. 1. Two configurations are studied (i) a configuration made of one piezoelectric element bonded on the elastic plate referred as a *bilayer configuration* and (ii) a configuration made of an elastic plate sandwiched between two identical piezoelectric elements referred as a *sandwich structure*. The $x - y$ plane is coincident with the elastic plate mid-plane. We denote by A_e the mid-plane occupied by the elastic plate and by A_p the mid-plane of the piezoelectric element. It is assumed that the piezoelectric elements or actuators are perfectly glued to the carrying deformable structure. The axis z is the thickness coordinate for both piezoelectric actuators and elastic plate. The plate thickness is denoted by h_e and that of the piezoelectric element is h_p. They are supposed constant. The elastic plate as well as the piezoelectric elements are materially homogeneous and either orthotropic or transversally isotropic with respect to the z-axis (in particular, the piezoelectric actuators are polarized along the thickness direction). In addition, the top and bottom faces of each piezoelectric element are covered by a conductive metallic electrode with negligible mechanical properties, the lateral surfaces are bare.

In order to derive an efficient and accurate two-dimensional model of the present composite plate accounting for the direct and inverse electromechanical coupling, we assume some hypotheses for the distribution of the electromechanical fields as function of the thickness coordinate.

3.1 Mechanical field distribution for the elastic plate.

The elastic displacement field for the plate is supposed to be of the form

$$\mathbf{u}^{(e)} = \left[U_{\alpha}^{(e)} - z w_{,\alpha}^{(e)} + f\left(z\right)\gamma_{\alpha}\right]\mathbf{e}_{\alpha} + w^{(e)}\mathbf{e}_{3}\ , \tag{6}$$

The summation over the index $\alpha \in \{1,2\}$ is applied. In Eq. (6), U_{α} represents the *mid-plane displacement component*, w is the *deflection* along the thickness direction and γ_{α} hold for the *shearing function*. All the functions are defined at the mid-plane coordinate $(x,y,0)$. The function $f(z)$ of the thickness coordinate is given by $f(z) = \frac{h_e}{\pi}\sin\left(\frac{\pi}{h_e}z\right)$ [8,11].

3.2 Electromechanical field distribution for the piezoelectric actuators.

The standard Love-Kirchhoff kinematics for the elastic displacement is considered. It is written as

$$\mathbf{u}^{(p)} = \left[U_{\alpha}^{(p)} - z w_{,\alpha}^{(p)}\right]\mathbf{e}_{\alpha} + w^{(p)}\mathbf{e}_{3}\ . \tag{7}$$

The shear correction function, as defined for the elastic layer, is not used for the piezoelectric part because the piezoelectric patches are supposed to be very thin.

A layerwise quadratic distribution of the electric potential is considered and given by

$$\phi = 2\frac{z_p}{h_p}V + P(z_p)\psi \quad \text{with} \quad z_p = z - z_0\ , \tag{8}$$

where $V\left(x,y,t\right)$ is the applied electric potential such as $\phi\left(z_p = +h_p/2\right) = +V$ and $\phi\left(z_p = -h_p/2\right) = -V$, z_p is the local thickness coordinate with respect to the actuator mid-plane and $z_0 = \frac{1}{2}\left(h_p + h_e\right)$ the coordinate of the mid-plane of the piezoelectric element. The second term in Eq. (8) is referred as the induced electric potential by elastic deformation in the piezoelectric element [8,9]. The function $P(z_p)$ is defined by $P(z_p) = z_p^2 - \left(\frac{h_p}{2}\right)^2$.

Remarks : The above description concerns the bilayer configuration (one piezoelectric element), however, in the case of the sandwich configuration for the lower piezoelectric element we must change V into $-V$ in Eq. (8) and z_0 into $-z_0$. We must distinguish the electric potential for the lower actuator denoted by $\phi^{(-)}$ and the electric potential distribution for the upper piezoelectic actuator given by $\phi^{(+)}$ in Eq. (8).

3.3 Continuity conditions at the layer interfaces.

The continuity of the elastic displacement at the interface between the elastic plate and the piezoelectric elements must be fullfilled at $z = +h_e/2$ (and at $z = -h_e/2$ in the case of the sandwich configuration). These continuity conditions read as

$$w^{(p)} = w^{(e)} = w \ , \tag{9a}$$

$$U_\alpha^{(p)} = U_\alpha^{(e)} + \frac{h_e}{\pi}\gamma_\alpha \ . \tag{9b}$$

In the case of the sandwich configuration a third condition identical to Eq. (9b) is also considered by changing h_e into $-h_e$.

3.4 Composite plate state field.

When hypotheses on the 3D distribution of the mechanical displacements and electric potential are given as a function of the following in-plane fields

$$\mathcal{W} = [\mathbf{U}, w, \boldsymbol{\gamma}, \psi, V] \ , \tag{10}$$

the strain tensor for the elastic plate can be written as

$$\mathbf{S}^{(e)} = \left(S_{\alpha\beta}^{(0)} + zS_{\alpha\beta}^{(1)} + f(z)S_{\alpha\beta}^{(2)}\right)\mathbf{e}_\alpha \otimes \mathbf{e}_\beta + \left(\frac{1}{2}f'(z)\gamma_\alpha\right)\mathbf{e}_\alpha \otimes \mathbf{e}_3 \ , \tag{11}$$

and for the piezoelectric element we have

$$\mathbf{S}^{(p)} = \left(S_{\alpha\beta}^{(0)} + zS_{\alpha\beta}^{(1)} + \frac{h_e}{\pi}S_{\alpha\beta}^{(2)}\right)\mathbf{e}_\alpha \otimes \mathbf{e}_\beta \ , \tag{12}$$

by using the continuity condition, Eq. (9b), the electric field within the piezoelectric element takes the form

$$\mathbf{E} = [P(z_p)E_\alpha]\,\mathbf{e}_\alpha + [E_3 - z_p\psi]\,\mathbf{e}_3 \ . \tag{13}$$

We have introduced the following generalized strain tensors

$$S_{\alpha\beta}^{(0)} = U_{(\alpha,\beta)}^{(e)} \ , \qquad S_{\alpha\beta}^{(1)} = -w_{,\alpha\beta} \ , \qquad S_{\alpha\beta}^{(2)} = \gamma_{(\alpha,\beta)} \ , \tag{14}$$

and the electric fields

$$E_\alpha = -\psi_{,\alpha} \ , \qquad E_3 = -2\frac{V}{h_p} \ . \tag{15}$$

Hence, the 3D distribution of mechanical strains and electric fields is determined by the set of generalized electromechanical fields

$$\mathcal{S} = \{S^{(0)}_{\alpha\beta}, S^{(1)}_{\alpha\beta}, S^{(2)}_{\alpha\beta}, E_\alpha, E_3\} \; . \tag{16}$$

We denote by $\mathcal{W}$ the functional space of compatible electromechanical kinematic fields of the reduced plate model. The fields defined by the sets (10) and (16) are said *compatible* if they are related through the compatibility relations (14) for the mechanical deformations and (15) for the electric fields which verify the essential boundary conditions for the elastic displacement and electric potential.

4 Equations for the piezoelectric composite

4.1 Variational formulation of the plate model

The equations of the present piezoelectric plate model are deduced by taking the first variation of the variational functional stated in Section 2 and by using the approximations for the elastic displacement and electric field.
On integrating over the thickness of the elastic plate and piezoelectric actuators, the dependence of the fields upon the thickness coordinate z is then rubbed out. After straighforward algebraic manipulations assuming independent variations of the generalized kinematical fields defined by Eq. (10). The variational formulation for the reduced plate model can be recast into the sum of variation contributions

$$-\delta U + \delta W_1 + \delta W_2 = 0 \; . \tag{17}$$

The different virtual works are defined on the mid-plan surface A_e of the elastic plate and mid-plan surface of the piezoelectric elements and also on the plate contour.

a - The first part holds for the variation of the plate model free energy written as

$$\begin{aligned} \delta U = \int_{A_e} \{ & N_{\alpha\beta}\delta S^{(0)}_{\alpha\beta} + M_{\alpha\beta}\delta S^{(1)}_{\alpha\beta} + \hat{R}_{\alpha\beta}\delta S^{(2)}_{\alpha\beta} + Q_\alpha \delta\gamma_\alpha \\ & - \mathcal{D}_\alpha \delta E_\alpha + \mathcal{D}_3 \delta\psi + q\delta V \} \, da \; . \end{aligned} \tag{18}$$

The generalized stresses $N_{\alpha\beta}$, $M_{\alpha\beta}$, $\hat{R}_{\alpha\beta}$, the generalized electric inductions $\mathcal{D}_\alpha$, $\mathcal{D}_3$ and the generalized density of electric charge q are defined (in the case of the

sandwich configuration) as

$$N_{\alpha\beta} = N_{\alpha\beta}^{(e)} + Y(\mathbf{X})\left(N_{\alpha\beta}^{(+)} + N_{\alpha\beta}^{(-)}\right) , \tag{19a}$$

$$M_{\alpha\beta} = M_{\alpha\beta}^{(e)} + Y(\mathbf{X})\left(M_{\alpha\beta}^{(+)} - M_{\alpha\beta}^{(-)}\right) , \tag{19b}$$

$$\hat{R}_{\alpha\beta} = R_{\alpha\beta}^{(e)} + \frac{h_e}{\pi} Y(\mathbf{X})\left(N_{\alpha\beta}^{(+)} - N_{\alpha\beta}^{(-)}\right) , \tag{19c}$$

$$\mathcal{D}_\alpha = \hat{D}_\alpha^{(+)} + \hat{D}_\alpha^{(-)} , \tag{19d}$$

$$\mathcal{D}_3 = \hat{D}_3^{(+)} - \hat{D}_3^{(-)} , \tag{19e}$$

$$q = q^{(+)} - q^{(-)} . \tag{19f}$$

It is worthwhile noting that for the bilayer configuration only the contributions of the upper piezoelectric actuator are involved in the above resultant definitions. In Eq. (19) the function $Y(\mathbf{X})$ is the index function defined as : $Y(\mathbf{X})$=1 if $\mathbf{X}$=$(x, y) \in A_p$ and $Y(\mathbf{X})$=0 otherwise. The resultants are computed using the 3D stress and electric displacement (see Eq. (5)) as follows

1) for the elastic plate

$$\left(N_{\alpha\beta}^{(e)}, M_{\alpha\beta}^{(e)}, R_{\alpha\beta}^{(e)}\right) = \int_{-h_e/2}^{+h_e/2} (1, z, f(z))\, \sigma_{\alpha\beta}^{(e)} dz , \tag{20a}$$

$$Q_\alpha = \int_{-h_e/2}^{+h_e/2} \frac{1}{2} f'(z) \sigma_{\alpha 3}^{(e)} dz , \tag{20b}$$

2) for the piezoelectric actuators

$$\left(N_{\alpha\beta}^{(+)}, M_{\alpha\beta}^{(+)}\right) = \int_{h_e/2}^{h_e/2+h_p} (1, z)\, \sigma_{\alpha\beta}^{(+)} dz , \tag{21a}$$

$$\hat{D}_\alpha^{(+)} = \int_{h_e/2}^{h_e/2+h_p} P(z_p)\, D_\alpha^{(+)} dz , \tag{21b}$$

$$\left(q^{(+)}, \hat{D}_3^{(+)}\right) = \int_{h_e/2}^{h_e/2+h_p} (1, 2z_p)\, D_3^{(+)} dz . \tag{21c}$$

The resultants for the lower piezoelectric actuator are deduced from those of the upper one by changing the superscript $(+)$ into $(-)$ and the segment of integration is $[-h_e/2 - h_p, -h_e/2]$.

b - The second part in the variational formulation (17) represents the virtual work of the body forces and electromechanical loads prescribed to the elastic plate and piezoelectric actuators. This virtual work can take a linear form on the set $\delta\mathcal{W}$ of the space defined by Eq. (10)

$$\delta W_1 = \int_{A_e} \left(b_\alpha \delta U_\alpha^{(e)} + b_T \delta w + \hat{m}_\alpha \delta\gamma_\alpha\right) da + \int_{A_p} \bar{q} \delta V\, da , \tag{22}$$

where $\mathbf{b}$ is the surface density of forces in the mid-plane, b_T is the surface density

of normal forces and $\hat{\mathbf{m}}$ is a density of moment per unit of area including eventually the inertial terms and $\bar{q}$ is the surface density of electric charges applied to the piezoelectric elements faces.

c - The last term in Eq. (17) denotes the virtual work of the forces and moments applied to the plate contour given by

$$\delta W_2 = \int_{\mathcal{C}} \left(F_\alpha \delta U_\alpha^{(e)} + \hat{T} \delta w - M_f \left(\delta w_{,n} \right) + C_\alpha \delta \gamma_\alpha \right) d\ell - \sum_k Z_k \delta w_k \ , \tag{23}$$

where $\mathbf{F}$ and $\hat{T}$ are force densities per unit of length, M_f and $\mathbf{C}$ are torques densities per unit of length defined along the contour $\mathcal{C}$ of the plate with $\mathbf{n}$ the unit outward normal to $\mathcal{C}$. At last, Z_k are transverse forces applied at the angular points of the contour boundary.

Remarks - The inertial contributions due to the acceleration forces are computed from the kinetic energy. The surface density of forces are splitted into the mechanical forces and inertial forces as $\mathbf{b} = \mathbf{f} + \mathbf{f}^{(I)}, b_T = p + p^{(I)}, \hat{\mathbf{m}} = \mathbf{m} + \mathbf{m}^{(I)}, \hat{T} = T + T^{(I)}$. The inertial contributions are then given by $f_\alpha^{(I)} = -\Gamma_\alpha^{(U)}, p^{(I)} = -\Gamma^{(w)}$, $m_\alpha^{(I)} = -\Gamma_\alpha^{(\gamma)}$ and $T^{(I)} = \hat{\Gamma}^{(w)}$.

The exact forms of the acceleration or inertial forces corresponding to the equations of motion according to two configurations are

(i) - *Bilayer configuration*

$$\Gamma_\alpha^{(U)} = I_0 \left(\mathbf{X} \right) \ddot{U}_\alpha - I_1 \left(\mathbf{X} \right) \ddot{w}_{,\alpha} + J_1 \left(\mathbf{X} \right) \ddot{\gamma}_\alpha \ , \tag{24a}$$

$$\Gamma^{(w)} = I_1 \left(\mathbf{X} \right) \ddot{U}_{\alpha,\alpha} + I_0 \left(\mathbf{X} \right) \ddot{w} - I_2 \left(\mathbf{X} \right) \ddot{w}_{,\alpha\alpha} + J_2 \left(\mathbf{X} \right) \ddot{\gamma}_{\alpha,\alpha} \ , \tag{24b}$$

$$\Gamma_\alpha^{(\gamma)} = J_1 \left(\mathbf{X} \right) \ddot{U}_\alpha - J_2 \left(\mathbf{X} \right) \ddot{w}_{,\alpha} + J_3 \left(\mathbf{X} \right) \ddot{\gamma}_\alpha \ , \tag{24c}$$

$$\hat{\Gamma}^{(w)} = \left[-I_1 \left(\mathbf{X} \right) \ddot{U}_\alpha + I_2 \left(\mathbf{X} \right) \ddot{w}_{,\alpha} - J_2 \left(\mathbf{X} \right) \ddot{\gamma}_\alpha \right] n_\alpha \ , \tag{24d}$$

where the different inertial moments are given by

$$\begin{aligned}
I_\ell \left(\mathbf{X} \right) &= I_\ell^{(e)} + Y \left(\mathbf{X} \right) I_\ell^{(p)} \quad \text{with} \quad \ell \in \{0, 1, 2\} \ , \\
J_1 \left(\mathbf{X} \right) &= J_1^{(e)} + Y \left(\mathbf{X} \right) \tfrac{h_e}{\pi} I_0^{(p)} \ , \\
J_2 \left(\mathbf{X} \right) &= J_2^{(e)} + Y \left(\mathbf{X} \right) \tfrac{h_e}{\pi} I_1^{(p)} \ , \\
J_3 \left(\mathbf{X} \right) &= J_3^{(e)} + Y \left(\mathbf{X} \right) \left(\tfrac{h_e}{\pi} \right)^2 I_0^{(p)} \ ,
\end{aligned}$$

and where we have defined the inertial moments of different order as

$$\left(I_0^{(e)}, I_1^{(e)}, I_2^{(e)}, J_1^{(e)}, J_2^{(e)}, J_3^{(e)}\right) = \int_{-h_e/2}^{+h_e/2} \rho_e \left(1, z, z^2, f\left(z\right), zf\left(z\right), f\left(z\right)^2\right) dz \,,$$

$$\left(I_0^{(p)}, I_1^{(p)}, I_2^{(p)}\right) = \int_{h_e/2}^{h_e/2+h_p} \rho_p \left(1, z, z^2\right) dz \,. \tag{25}$$

(ii) - *Sandwich configuration*

In the case of the sandwich configuration the equations (25) are also considered by changing $I_\ell^{(p)}$ by $2I_\ell^{(p)}$ ($\ell \in \{0,1,2\}$) and with $I_1\left(\mathbf{X}\right) = J_1\left(\mathbf{X}\right) = 0$.

4.2 Balance equations

The balance equations and the natural boundary conditions are derived by using classical arguments of variational calculus in the functional space $\mathcal{W}$ of compatible kinematical fields. The balance equations are then given by

$$N_{\alpha\beta,\beta} + b_\alpha = 0 \,, \tag{26a}$$
$$M_{\alpha\beta,\alpha\beta} + b_T = 0 \,, \tag{26b}$$
$$\hat{R}_{\alpha\beta,\beta} - Q_\alpha + \hat{m}_\alpha = 0 \,. \tag{26c}$$

In addition, we have for the piezoelectric actuators

$$\mathcal{D}_{\alpha,\alpha} - \mathcal{D}_3 = 0 \,, \tag{27a}$$
$$q - \bar{q} = 0 \,. \tag{27b}$$

The natural boundary conditons are derived for all the admissible variations of the field defined in the space (10)

$$\left[N_{\alpha\beta}n_\beta - F_\alpha\right] \delta U_\alpha = 0 \,, \tag{28a}$$
$$\left[\left(\tau_\alpha M_{\alpha\beta}n_\beta\right)_{,s} - n_\alpha M_{\alpha\beta,\beta} - \hat{\Gamma}^{(w)} + T\right] \delta w + \left[n_\alpha M_{\alpha\beta}n_\beta - M_f\right] \delta w_{,n} = 0 \,, \tag{28b}$$
$$\left[\hat{R}_{\alpha\beta}n_\beta - C_\alpha\right] \delta\gamma_\alpha = 0 \,, \tag{28c}$$
$$\left[\mathcal{D}_\alpha n_\alpha\right] \delta\psi = 0 \,. \tag{28d}$$

The vector τ is the unit tangent vector to the contour $\mathcal{C}$ and s is the curvilinear coordinate along the plate contour. The condition at the angular points a_k of the contour is given by $\left[\!\left[\tau_\alpha M_{\alpha\beta}n_\beta - Z_k\right]\!\right]_{a_k} \delta w_k = 0$. Since the lateral boundary of the piezoelectric actuators is bare (no electrode) there is no electric charge density applied to the actuator contour.

Remarks

1) - It is worthwhile noticing that the first two equations (26) are similar to those

of the Love-Kirchhoff first-order theory of elastic thin plates. The third equation governs the shearing effect. The additional equations (27) are deduced from the conservation law of the electric charge or the Gauss equation.
2) - In the case of an electric potential applied to the piezoelectric element faces, the electric charge balance equation (27b) does not exist and it is replaced by the essential boundary condition on the electric potential (V given).

5 Constitutive equations

The constitutive equations for the present piezoelectric composite plate model are deduced from the 3D constitutive equations for piezoelectric and elastic materials stated in Section 2. The global plate constitutive equations are computed from the resultants defined by Eqs (20) and (21) and can be put in matrix form according to the two configurations.

(i) - Bilayer configuration

$$\begin{bmatrix} \mathcal{D} \\ \mathbf{Q} \end{bmatrix} = \begin{bmatrix} K^{DE} & 0 \\ 0 & K^{Q\gamma} \end{bmatrix} \begin{bmatrix} \mathbf{E} \\ \boldsymbol{\gamma} \end{bmatrix} , \tag{29}$$

$$\begin{bmatrix} \mathbf{N} \\ \mathbf{M} \\ \hat{\mathbf{R}} \\ q \\ \mathcal{D}_3 \end{bmatrix} = \begin{bmatrix} K^{NU} & K^{Nw} & K^{N\gamma} & \left(K^{NV}\right)^T & 0 \\ K^{Nw} & K^{Mw} & K^{M\gamma} & \left(K^{MV}\right)^T & \left(K^{M\psi}\right)^T \\ K^{N\gamma} & K^{M\gamma} & K^{R\gamma} & \left(K^{RV}\right)^T & 0 \\ K^{NV} & K^{MV} & K^{RV} & K^{qV} & 0 \\ 0 & K^{M\psi} & 0 & 0 & K^{D\psi} \end{bmatrix} \begin{bmatrix} \mathbf{S}^{(0)} \\ \mathbf{S}^{(1)} \\ \mathbf{S}^{(2)} \\ V \\ \psi \end{bmatrix} . \tag{30}$$

(ii) - Sandwich configuration

$$\begin{bmatrix} \mathbf{N} \\ \mathcal{D} \\ \mathbf{Q} \end{bmatrix} = \begin{bmatrix} K^{NU} & \left(K^{NE}\right)^T & 0 \\ K^{NE} & K^{DE} & 0 \\ 0 & 0 & K^{Q\gamma} \end{bmatrix} \begin{bmatrix} \mathbf{S}^{(0)} \\ \mathbf{E} \\ \boldsymbol{\gamma} \end{bmatrix} , \tag{31}$$

$$\begin{bmatrix} \mathbf{M} \\ \hat{\mathbf{R}} \\ q \\ \mathcal{D}_3 \end{bmatrix} = \begin{bmatrix} K^{Mw} & K^{M\gamma} & \left(K^{MV}\right)^T & \left(K^{M\psi}\right)^T \\ K^{M\gamma} & K^{R\gamma} & \left(K^{RV}\right)^T & 0 \\ K^{MV} & K^{RV} & K^{qV} & 0 \\ K^{M\psi} & 0 & 0 & K^{D\psi} \end{bmatrix} \begin{bmatrix} \mathbf{S}^{(1)} \\ \mathbf{S}^{(2)} \\ V \\ \psi \end{bmatrix}. \tag{32}$$

where all the components of the block matrices (not given here for a sake of simplicity) depend on the elastic plate and piezoelectric actuators thicknesses and material constants of the constituents (elasticity, piezoelectricity and dielectric permittivity). We have set the following resultant vectors (using the Voigt notation)

$$\mathbf{N} = \begin{bmatrix} N_1 \\ N_2 \\ N_6 \end{bmatrix}, \ \mathbf{M} = \begin{bmatrix} M_1 \\ M_2 \\ M_6 \end{bmatrix}, \ \hat{\mathbf{R}} = \begin{bmatrix} \hat{R}_1 \\ \hat{R}_2 \\ \hat{R}_6 \end{bmatrix}, \ \mathbf{Q} = \begin{bmatrix} Q_1 \\ Q_2 \end{bmatrix}, \ \mathcal{D} = \begin{bmatrix} \mathcal{D}_1 \\ \mathcal{D}_2 \end{bmatrix}. \tag{33}$$

In addition, we define generalized strain vectors and electric field vector as follows

$$\mathbf{S}^{(\ell)} = \begin{bmatrix} S_1^{(\ell)} \\ S_2^{(\ell)} \\ S_6^{(\ell)} \end{bmatrix} \text{ with } \quad \ell \in \{0, 1, 2\}, \quad \boldsymbol{\gamma} = \begin{bmatrix} \gamma_1 \\ \gamma_2 \end{bmatrix}, \ \mathbf{E} = \begin{bmatrix} E_1 \\ E_2 \end{bmatrix}. \tag{34}$$

Remarks
1) - It is observed that there is no coupling between membrane deformation and plate deflection for the sandwich configuration.
2) - Some components of the block matrices can be zero due to the particular material symmetry or the zero material constants.

6 Solution to the plate under cylindrical bending

Here, we place our attention to the problem of a piezoelectric element bonded on an elastic plate *simply supported* under *cylindrical bending* as depicted in Fig. 2. In the cylindrical bending situation, the electromechanical state variables do not depend on the y variable. Accordingly, the displacement u_2 does not play any role in the problem, so that $U_2 = 0$ and $\gamma_2 = 0$.
The plate suffers a *surface density of normal force* applied to the top face and an *electric potential* is applied to the top and bottom faces of the piezoelectric patches.

It is supposed that there is no shear traction and surface density of moment on the plate faces, i.e. $f_\alpha = 0$ and $\hat{m}_\alpha = 0$.

In this particular situation, the equations of motion take the simplified forms

$$N_{,x} = \Gamma^{(U)} \,, \tag{35a}$$

$$M_{,xx} + p = \Gamma^{(w)} \,, \tag{35b}$$

$$\hat{R}_{,x} - Q = \Gamma^{(\gamma)} \,, \tag{35c}$$

$$\mathcal{D}_{,x} - \mathcal{D}_3 = 0 \,. \tag{35d}$$

The equation (27b) does not exist since the electric potential V is given on the piezoelectric actuator faces.
The electromechanical loads are expanded in a Fourier series over the segment $[0, L]$ and are written as

$$(p(x,t), V(x,t)) = \sum_{n=1}^{N} (S_n, V_n) \sin(\lambda_n x)\, e^{i\omega t} \,, \tag{36}$$

with $\lambda_n = \frac{n\pi}{L}$ and S_n and V_n are the Fourier coefficients of the applied surface density of force and electric potential, respectively. Moreover, we set $V(x) = Y(x)\, V_0$ with $Y(x)$ the index function defined by $Y(x) = H(x - L_1) - H(x - L_2)$, where $H(x)$ is the Heaviside unit function ($H(x) = 1$ if $x \geq 0$ and $H(x) = 0$ otherwise) and V_0 is the uniform electric potential, where L_1 and L_2 are the abscissa of the patch ends (see Fig. 2).

We look for solutions to the equations of motion as Fourier series given by

$$\begin{gathered}(U(x,t), w(x,t), \gamma(x,t), \psi(x,t)) = \\ \sum_{n=0}^{N} (U_n \cos(\lambda_n x), W_n \sin(\lambda_n x), \Gamma_n \cos(\lambda_n x), \Psi_n sin(\lambda_n x))\, e^{i\omega t} \,.\end{gathered} \tag{37}$$

We notice that Eq. (37) satisfies the boundary conditions for the cylindrical bending configuration. Now, we substitute the load equations (36) and solution equations (37) into the set of linearly coupled differential equations. The next step consists of projecting the equations on the Fourier base $\{\cos(\lambda_m x), \sin(\lambda_m x)\}$ and integrating over the segment $[0, L]$. So, the dependency upon the x variable is cancelled out and this leads to a set of linear algebraic equations for the Fourier coefficients of the displacement and electric potential $\{U_n, W_n, \Gamma_n, \Psi_n; n \in [1, ..., N]\}$, where N is the number of terms retained in the series to ensure the convergence.

(i) - *Bilayer configuration*

$$\begin{bmatrix} \mathbb{A}_{11} & \mathbb{A}_{12} & \mathbb{A}_{13} & \mathbb{O} \\ \mathbb{A}_{21} & \mathbb{A}_{22} & \mathbb{A}_{23} & \mathbb{A}_{24} \\ \mathbb{A}_{31} & \mathbb{A}_{32} & \mathbb{A}_{33} & \mathbb{O} \\ \mathbb{O} & \mathbb{A}_{42} & \mathbb{O} & \mathbb{A}_{44} \end{bmatrix} \begin{bmatrix} \mathbf{U} \\ \mathbf{W} \\ \mathbf{\Gamma} \\ \mathbf{\Psi} \end{bmatrix} = \begin{bmatrix} \mathbf{B_1} \\ \mathbf{B_2} \\ \mathbf{B_3} \\ \mathbf{0} \end{bmatrix} \tag{38}$$

(ii) - *Sandwich configuration*

$$\overline{\mathbb{A}}_{11}\mathbf{U} = \mathbf{0} \quad \text{and} \quad \begin{bmatrix} \overline{\mathbb{A}}_{22} & \overline{\mathbb{A}}_{23} & \overline{\mathbb{A}}_{24} \\ \overline{\mathbb{A}}_{32} & \overline{\mathbb{A}}_{33} & \mathbb{O} \\ \overline{\mathbb{A}}_{42} & \mathbb{O} & \overline{\mathbb{A}}_{44} \end{bmatrix} \begin{bmatrix} \mathbf{W} \\ \mathbf{\Gamma} \\ \mathbf{\Psi} \end{bmatrix} = \begin{bmatrix} \overline{\mathbf{B}}_\mathbf{2} \\ \overline{\mathbf{B}}_\mathbf{3} \\ \mathbf{0} \end{bmatrix} \tag{39}$$

The vectors $\mathbf{B}$ and $\overline{\mathbf{B}}$ of N dimension contain the Fourier coefficients of the electromechanical loads. The block matrices $\mathbb{A}$ and $\overline{\mathbb{A}}$ are $N \times N$ matrices and $\mathbb{O}$ is $N \times N$ zero matrix. The vectors $\mathbf{U}$, $\mathbf{W}$, $\mathbf{\Gamma}$ and $\mathbf{\Psi}$ contain the first N Fourier coefficients. All these aforementionned quantities are specified in Appendix A.

7 Numerical results and comparisons

The numerical computations using the present approach are carried out for a piezoelectric patch made of PZT-4 ceramics perfectly bonded on a composite plate made of graphite fibers aligned along x direction in epoxy matrix (see Tables 1 and 2 for the material properties with $C^E_{\alpha\beta}$ expressed in GPa, $e_{i\alpha}$ in C/m^2 and ϵ^S_{ij} in nF/m). The geometrical parameters of the problem are $L = 0.15$m, $L/h_e = 50$, $L/(L_2 - L_1) = 5$ and $h_e/h_p = 3$. Only the *actuator function* is examinated with an applied electric potential of the order $V_0 = 100$ Volts ($S_n = 0$ or $p = 0$).

A first set of numerical computations for the bilayer and sandwich configurations (two identical piezoelectric elements symmetrically bonded to the elastic plate) leads to the global deflection as function of $x \in [0, L]$ for a piezoelectric patch located at the plate center (Fig. 3a and Fig. 4a) and located at x=$L/4$ (Fig. 5b and Fig. 6b). The solid-line curve corresponds to the present model, the dashed line curve to the simplified model (no shear correction and no quadratic term in the electric potential). In spite of the slenderness ratio L/h_e=50, the discrepancy for the maximum deflection between the present model and the simplified model is respectively about 3.5% for the bilayer configuration and about 5.7% for the sandwich configuration if the piezoelectric patches are located at x=$L/2$. It is observed that the

longitudinal displacement as function of x (Fig. 5a and Fig. 6a) is linear within the piezoelectric parts and it corresponds to the patch extension; in the elastic part, it is obviously constant. The longitudinal displacement at x=L, depicted in Fig. 3b and Fig. 4b, shows a linear variation over the elastic plate thickness. The electromechanical field distributions computed at the center of the patch exhibit jumps at z=$\pm h_e/2$ in Fig. 3c and Fig. 4c for the longitudinal stress and in Fig. 3d and Fig. 4d for the normal electric induction. The latter curve is layerwise constant in the piezoelectric actuators.

Some characteristic values in physical units $w^*(x = \frac{L}{2}, z = 0)$ for the deflection, $u^*(x = L, z = \frac{h_e}{2})$ for the axial displacement, $\sigma_{11}^*(x = \frac{L}{2}, z = \frac{h_e}{2})$ for the axial stress and $D_3^*(x = \frac{L}{2}, z = \frac{h_e}{2})$ for the normal component of the electric displacement are given in Tables 3 and 4. In particular, we observe a maximum of the deflection, when applying an electric potential of 100 Volts, of the order of $26.3\,\mu$m for x=$L/2$ and only $8.2\,\mu$m for x=$L/4$ in the case of the sandwich configuration. In the case of the bilayer configuration the maximum of deflection is reduced to $14.2\,\mu$m for x=$L/2$ and $5.8\,\mu$m for x=$L/4$.

8 Plate vibrations and frequency spectra

The second set of numerical results concerns the frequencies of vibration modes of the elastic plate (i) equipped with a piezoelectric actuator and (ii) sandwiched between two piezoelectric elements. The modal frequencies for the closed circuit condition are listed in Tables 5 and 6 for the first eight flexural modes and the first two axial modes.

The numerical results for the sandwich configuration show that there is no difference between the present model and the simplified model for the axial frequencies because the shear correction does not play any role in these modes. Nevertheless, for the flexural frequencies (see Table 6), the discrepancy is quite significant (more than 20% for n=8).

In the case of the bilayer configuration with x=$L/2$, the difference between the simplified model and the present model is over than 2% for the second axial frequency and more than 20% for the eighth flexural frequency.

Comparing both results of Tables 5 and 6, we can observe that the flexural frequencies for the sandwich configuration are smaller than those for the bilayer situation. This is due to the modification of the flexural stiffness of the composite plate.

Furthermore, comments on the influence of the piezoelectric actuator position can be reported. Indeed, it is observed in Table 5 that the piezoelectric actuator located at $x = L/4$ affects mostly the modes number 2, 4 and 8 leading to lower natural

frequencies. The same comment holds for the sandwich configuration (Table 6). Insofar as the axial modes are concerned, it is not so obvious. Piezoelectric element position has a greater influence on the modal frequencies. In fact, for the bilayer configuration the position at x=L/4 tends to increase the modal frequencies (see Table 5). For the sandwich configuration the same remark holds except for the first mode because the flexural and axial modes are not coupled.

If we suppose that the electric potential applied to the piezoelectric elements is harmonic in time $V = V_0 e^{i\omega t}$. The set of linear equations to be solved is still Eqs. (38) and (39) but with $S_n = 0$ and $V_n \neq 0$ and with non-zero circular frequency (ω=2$\pi\nu$). The numerical results for the spectrum of the flexural mode is shown in Figs. 7 and 8 where we notice that the simplified model overestimates the higher resonant frequencies in comparison to the refined model. It is worthwhile noting that the modal frequencies listed in Tables 5 and 6 correspond to those of the peaks of Figs. 7 and 8.

9 Conclusion

In the present work, we have investigated the modelling of static and dynamic responses of an elastic structure (plate) equipped with piezoelectric elements. We have proposed an accurate and efficient approximation for the elastic displacement including shear correction function and a quadratic distribution of the electric potential through the piezoelectric layer. The present approach accurately predicts the global (elongation, deflection, frequencies) and local (field distribution) responses of the composite structures. A number of numerical tests has been proposed for two cases (i) a bilayer configuration with one piezoelectric element and (ii) piezoelectric actuators symmetrically placed on both sides of the elastic plate. The study accounts for the influence of the stiffness and inertial contribution of the piezoelectric elements on the local and global responses of the structure. They play non negligible role. One of the important difficulties is that the piezoelectric patches introduced material and geometrical discontinuities. In the present work, the equations of motion have been solved by projecting them on the Fourier base. Such a study of piezoelectric composites including active piezoelectric elements seems to be useful for structural control of elastic structures (vibration and shape) [12]. Extension to more refined models including nonlinear effects could be investigated in further works.

References

[1] T. Tani, T. Takagi and J. Qiu, *"Intelligent material systems : Application of functional material"*, Appl. Mech. Rev., 52, 505-521, 1998.

[2] D.A. Saravanos and P.R. Heyliger, *"Mechanics and computational models for laminated piezoelectric beams, plates and shells"*, Appl. Mech. Rev., 52, 305-320, 1999.
[3] E. Carrera, *"An improved Reissner-Mindlin-type model for the electromechanical analysis of multilayered plates including piezo-layer"*, J. Intell. Mat. Syst. Struct., 8, 232-248, 1997.
[4] H. Abramovich, *"Deflection control of laminated composite beams with piezoceramics layers - close-form solutions"*, Compos. Struct., 93, 217-231, 1998.
[5] J.M. Sloss, J.C. Bruch Jr., S. Adal and I.S. Sadek, *"Piezoelectric patch control using an integral equation approach"*, Thin-Walled Struct., 39, 45-63, 2001.
[6] J.S. Yang, *"Equation for thick elastic plates with partially electroded piezoelectric actuators and higher order electric fields"*, Smart Mater. Struct., 8, 73-82, 1999.
[7] I. Chopra, *"Review of state of art of smart structures and integrated systems"*, AIAA J., 40, 2145-2187, 2002.
[8] A. Fernandes and J. Pouget, *"An accurate modelling of piezoelectric plates. Single-layered plate"*, Arch. Appl. Mech., 71, 509-524, 2001.
[9] A. Fernandes and J. Pouget, *"Analytical and numerical approaches to piezoelectric bimorph"*, Int. J. Solids Struct., 40, 4331-4352, 2003.
[10] T. Ikeda, *"Fundamental of piezoelectricity*, Oxford University Press, Oxford, 1996.
[11] A. Fernandes and J. Pouget, *"An accurate modelling of piezoelectric multi-layer plates"*, Eur. J. Mech. A/Solids, 21, 629-651, 2002.
[12] H. Irschik, *"A review on static and dynamic shape control of structures by piezoelectric actuation"*, Eng. Struct., 24, 5-11, 2002.

Appendix A - Fourier coefficients.

The present appendix gives the detailed components of the matrix form defined in Section 6 for the bilayer (Eq. (38)) and sandwich (Eq. (39)) configurations in the case of the cylindrical bending problem.

(i) - *Bilayer configuration*

For the bilayer configuration the components of the matrix $\mathbb{A}$ are

$$
\begin{aligned}
a_{11}^{mn} &= (I_0^{\prime(e)}\delta_{mn} + I_0^{\prime(p)} c_{00}^{mn})\Omega^2 - (Q_{11}^{\prime(p)} s_{11}^{mn} + \Lambda_n^2\, Q_{11}^{\prime(e)}\delta_{mn}) \\
a_{12}^{mn} &= -I_1^{\prime(p)} c_{01}^{mn}\, \Omega^2 + Z_0\, Q_{11}^{\prime(p)} s_{12}^{mn} \\
a_{13}^{mn} &= \tfrac{H_e}{\pi}(I_0^{\prime(p)} c_{00}^{mn}\, \Omega^2 - Q_{11}^{\prime(p)} s_{11}^{mn})
\end{aligned}
$$

$$
\begin{aligned}
a_{21}^{mn} &= -I_1^{\prime(p)} s_{01}^{mn}\Omega^2 + Z_0 Q_{11}^{\prime(p)} s_{21}^{mn} \\
a_{22}^{mn} &= \Big[(I_0^{\prime(e)} + \Lambda_n^2\, I_2^{\prime(e)})\delta_{mn} + I_0^{\prime(p)} s_{00}^{mn} + I_2^{\prime(p)} s_{02}^{mn}\Big]\, \Omega^2 \\
&\qquad - \Big[(D_{11}^{\prime(p)} + Z_0^2 Q_{11}^{\prime(p)}) s_{22}^{mn} + \Lambda_n^4 D_{11}^{\prime(e)}\delta_{mn}\Big] \\
a_{23}^{mn} &= -(\tfrac{H_e}{\pi} I_1^{\prime(p)} s_{01}^{mn} + \Lambda_n\, J_2^{'(e)}\delta_{mn})\Omega^2 + \tfrac{H_e}{\pi} Z_0 Q_{11}^{\prime(p)} s_{21}^{mn} + \Lambda_n^3 d_{11}^{\prime(e)}\delta_{mn} \\
a_{24}^{mn} &= E_{31}^{\prime} s_{20}^{mn}
\end{aligned}
$$

$$
\begin{aligned}
a_{31}^{mn} &= \tfrac{H_e}{\pi}(I_0^{\prime(p)} c_{00}^{mn}\Omega^2 - Q_{11}^{\prime(p)} s_{11}^{mn}) \\
a_{32}^{mn} &= -(\tfrac{H_e}{\pi} I_1^{\prime(p)} c_{01}^{mn} + \Lambda_n\, J_2^{\prime(e)}\delta_{mn})\Omega^2 + \tfrac{H_e}{\pi} Z_0 Q_{11}^{\prime(p)} s_{12}^{mn} + \Lambda_n^3\, d_{11}^{\prime(e)}\delta_{mn} \\
a_{33}^{mn} &= (J_3^{\prime(e)}\delta_{mn} + \tfrac{H_e^2}{\pi^2} I_0^{\prime(p)} c_{00}^{mn})\Omega^2 - [(\hat{A}_{55}^{\prime} + \Lambda_n^2\, \hat{D}_{11}^{\prime(e)})\delta_{mn} + \tfrac{H_e^2}{\pi^2} Q_{11}^{\prime(p)} s_{11}^{mn}]
\end{aligned}
$$

$$
\begin{aligned}
a_{42}^{mn} &= E_{31}^{\prime} s_{02}^{mn} \\
a_{44}^{mn} &= G_{11}^{\prime} c_{11}^{mn} + H_{33}^{\prime} s_{00}^{mn}
\end{aligned}
$$

and the components of the vector $\mathbf{B}$ are

$$
\begin{aligned}
b_1^m &= -2\Lambda_m e_{31}^{\prime}\hat{V}_m \\
b_2^m &= -\hat{S}_m + 2\Lambda_m^2 Z_0 e_{31}^{\prime}\hat{V}_m \\
b_3^m &= -\tfrac{2H_e}{\pi}\Lambda_m e_{31}^{\prime}\hat{V}_m
\end{aligned}
$$

In the above definitions we have set $\Lambda_n = \lambda_n h_0$ and $(H_a, Z_0) = \frac{1}{h_0}(h_a, z_0)$ with $(a = e)$ for the elastic plate and $(a = p)$ for the piezoelectric element . We have also introduced the dimensionless electromechanical and inertial variables and material constants :

$$
(\hat{U}_n, \hat{W}_n, \hat{\Gamma}_n) = \frac{C_{00}}{h_0^2}(U_n, W_n, h_0\Gamma_n);\ \hat{\Psi}_n = \frac{C_{00}\Psi_n}{E_0};\ \hat{V}_n = \frac{C_{00}V_n}{h_0^2 E_0};\ \hat{S}_n = \frac{S_n}{h_0}
$$

$$(I_0'^{(a)}, I_1'^{(a)}, I_2'^{(a)}, J_2'^{(a)}, J_3'^{(a)}) = \frac{1}{\rho_0 h_0^3}(h_0^2 I_0^{(a)}, h_0 I_1^{(a)}, I_2^{(a)}, J_2^{(a)}, J_3^{(a)});\ \Omega^2 = \frac{\rho_0 h_0^2}{C_{00}}\omega^2$$

$$(D_{11}'^{(a)}, d_{11}'^{(a)}, \hat{D}_{11}'^{(a)}, Q_{11}'^{(a)}, \hat{A}_{55}') = \frac{1}{h_0^3 C_{00}}(D_{11}^{(a)}, d_{11}^{(a)}, \hat{D}_{11}^{(a)}, h_0^2 Q_{11}^{(a)}, h_0^2 \hat{A}_{55});$$

$$e_{31}' = \frac{E_0 e_{31}}{C_{00}};\ E_{31}' = \frac{E_0 E_{31}}{h_0^3 C_{00}};\ G_{11}' = \frac{E_0^2 G_{11}}{h_0^5 C_{00}};\ H_{33}' = \frac{E_0^2 H_{33}}{h_0^3 C_{00}};$$

with the physical quantities

$$Q_{11}^{(a)} = h_a C_{11}^{(a)};\ D_{11}^{(a)} = \frac{h_a^3}{12} C_{11}^{(a)};\ d_{11}^{(a)} = \frac{2h_a^3}{\pi^3} C_{11}^{(a)};\ \hat{D}_{11}^{(a)} = \frac{h_a^3}{2\pi^2} C_{11}^{(a)};\ \hat{A}_{55} = \frac{h_e}{2} C_{55}^{(e)}$$

$$E_{31} = -\frac{h_p^3}{6} e_{31};\ G_{11} = \frac{h_p^5}{30}\epsilon_{11}^S;\ H_{33} = \frac{h_p^3}{3}\epsilon_{33}^S$$

where the constants C_{00}, h_0 and ρ_0 are respectively the constant elastic modulus, the thickness and mass density of references (elastic layer for numerical investigations) and for numerical convenience $E_0 = 10^{10}$ V/m.

Moreover we have set

$$s_{ij}^{mn} =< Y(X)\Lambda_m^i \sin(m\pi X)\,, \Lambda_n^j \sin(n\pi X) >$$
$$c_{ij}^{mn} =< Y(X)\Lambda_m^i \cos(m\pi X)\,, \Lambda_n^j \cos(n\pi X) > \quad \{i,j\} = \{0,1,2\}$$

with the operator $<\,,\,>$ is defined as $< f, g >= 2\int_0^1 f g\, dX$ with $X = \frac{x}{L}$

(ii) - *Sandwich configuration*

For the sandwich configuration the components of the matrix $\overline{\mathbb{A}}$ are

$$\overline{a}_{11}^{mn} = (I_0^{\prime(e)}\delta_{mn} + 2I_0^{\prime(p)}c_{00}^{mn})\Omega^2 - (2Q_{11}^{\prime(p)}s_{11}^{mn} + \Lambda_n^2 Q_{11}^{\prime(e)}\delta_{mn})$$

$$\begin{aligned}\overline{a}_{22}^{mn} &= \left[(I_0^{\prime(e)} + \Lambda_n^2\ I_2^{\prime(e)})\delta_{mn} + 2(I_0^{\prime(p)}s_{00}^{mn} + I_2^{\prime(p)}s_{02}^{mn})\right]\Omega^2 \\ &\qquad - \left[2(D_{11}^{\prime(p)} + Z_0^2 Q_{11}^{\prime(p)})s_{22}^{mn} + \Lambda_n^4 D_{11}^{\prime(e)}\delta_{mn}\right] \\ \overline{a}_{23}^{mn} &= -(\tfrac{2H_e}{\pi}I_1^{\prime(p)}s_{01}^{mn} + \Lambda_n\ J_2^{\prime(e)}\delta_{mn})\Omega^2 + \tfrac{2H_e}{\pi}Z_0 Q_{11}^{\prime(p)}s_{21}^{mn} + \Lambda_n^3 d_{11}^{\prime(e)}\delta_{mn} \\ \overline{a}_{24}^{mn} &= 2E_{31}^{\prime}s_{20}^{mn}\end{aligned}$$

$$\begin{aligned}\overline{a}_{32}^{mn} &= -(\tfrac{2H_e}{\pi}I_1^{\prime(p)}c_{01}^{mn} + \Lambda_n\ J_2^{\prime(e)}\delta_{mn})\Omega^2 + \tfrac{2H_e}{\pi}Z_0 Q_{11}^{\prime(p)}s_{12}^{mn} + \Lambda_n^3\ d_{11}^{\prime(e)}\delta_{mn} \\ \overline{a}_{33}^{mn} &= (J_3^{\prime(e)}\delta_{mn} + \tfrac{2H_e^2}{\pi^2}I_0^{\prime(p)}c_{00}^{mn})\Omega^2 - [(\hat{A}_{55}^{\prime} + \Lambda_n^2\ \hat{D}_{11}^{\prime(e)})\delta_{mn} + \tfrac{2H_e^2}{\pi^2}Q_{11}^{\prime(p)}s_{11}^{mn}]\end{aligned}$$

$$\begin{aligned}\overline{a}_{42}^{mn} &= 2E_{31}^{\prime}s_{02}^{mn} \\ \overline{a}_{44}^{mn} &= 2(G_{11}^{\prime}c_{11}^{mn} + H_{33}^{\prime}s_{00}^{mn})\end{aligned}$$

and the components of the vector $\overline{\mathbf{B}}$ are

$$\begin{aligned}\overline{b}_2^m &= -\hat{S}_m + 4\Lambda_m^2 Z_0 e_{31}^{\prime}\hat{V}_m \\ \overline{b}_3^m &= -\tfrac{4H_e}{\pi}\Lambda_m e_{31}^{\prime}\hat{V}_m\end{aligned}$$

List of Tables

List of Figures

Tables

	C_{11}^E	C_{12}^E	C_{33}^E	C_{13}^E	C_{44}^E	e_{31}	e_{33}	e_{15}	ϵ_{11}^S	ϵ_{33}^S
PZT-4	139.	77.8	115.	74.3	25.6	-5.2	15.1	12.7	13.06	11.51

Table 1
Material constants for the PZT4 ceramic (C_{ij}^E in [GPa], e_{ij} in [C/m^2] and ϵ_{ij}^S in [nF/m]).

	C_{11}^E	C_{12}^E	C_{22}^E	C_{23}^E	C_{55}^E	e_{31}	e_{33}	e_{15}	ϵ_{11}^S	ϵ_{33}^S
Comp.	134.86	5.1563	14.352	7.1329	5.654	0	0	0	0.031	0.0266

Table 2
Material constants for the graphite/epoxy composite (C_{ij}^E in [GPa] and ϵ_{ij}^S in [nF/m]).

	$x = L/2$		$x = L/4$	
	Simp. Model	Present Model	Simp. Model	Present Model
w^* **[μm]**	13.7399	14.2384	5.94668	5.80753
u^* **[μm]**	0.391476	0.40287	0.115113	0.110985
σ_{11}^* **[MPa]**	-1.70128	-1.73127	-1.62216	-1.67497
D_3^* **[mC/m^2]**	-2.90893	-2.96064	-2.92192	-2.98491

Table 3
Characteristic electromechanical values for the bilayer configuration (patch position at x=$L/2$ and x=$L/4$).

	$x = L/2$		$x = L/4$	
	Simp. Model	Present Model	Simp. Model	Present Model
w^* **[μm]**	24.8281	26.3238	8.47685	8.20863
u^* **[μm]**	0.56934	0.599314	0.130699	0.124644
σ_{11}^* **[MPa]**	-1.5523	-1.55115	-1.43574	-1.51824
D_3^* **[mC/m^2]**	-2.93339	-3.01699	-2.95253	-3.04228

Table 4
Characteristic electromechanical values for the sandwich configuration (patch position at x=$L/2$ and x=$L/4$).

		$x = L/2$		$x = L/4$	
		Simp. Model	Present Model	Simp. Model	Present Model
Flexural	n=1	603.96	598.48	608.79	604.29
	n=2	2770.2	2719.5	2474.9	2418.6
	n=3	5827.8	5570.8	5848.2	5595.7
	n=4	10894.	10163.	10163.	9434.2
	n=5	16695.	14987.	16461.	14783.
	n=6	24034.	20819.	24059.	20775.
	n=7	33056.	27478.	31799.	26251.
	n=8	42112.	33449.	41670.	32997.
Axial	n=1	39050.9	38754.6	46351.5	46106.4
	n=2	61855.9	60588.9	76485.9	77236.

Table 5
Modal frequencies in [Hz] for the bilayer configuration (patch position at x=$L/2$ and x=$L/4$).

		$x = L/2$		$x = L/4$	
		Simp. Model	Present Model	Simp. Model	Present Model
Flexural	n=1	539.86	532.52	550.79	544.88
	n=2	2751.3	2700.3	2432.2	2361.8
	n=3	5735.3	5447.4	5670.	5384.7
	n=4	10664.	9932.	9696.8	8948.1
	n=5	16883.	15041.	16598.	14812.
	n=6	23312.	20094.	24419.	20844.
	n=7	33800.	27814.	31825.	25953.
	n=8	41003.	32351.	42099.	32937.
Axial	n=1	39602.5	39602.5	27458.8	27458.8
	n=2	52365.9	52365.9	61855.9	61855.9

Table 6
Modal frequencies in [Hz] for the sandwich configuration (patch position at x=$L/2$ and x=$L/4$).

Figures

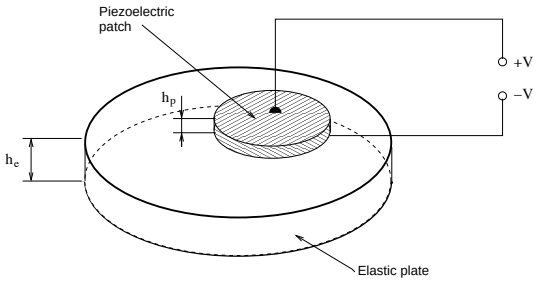

Fig. 1. Sketch of a piezoelectric element perfectly attached onto an elastic plate.

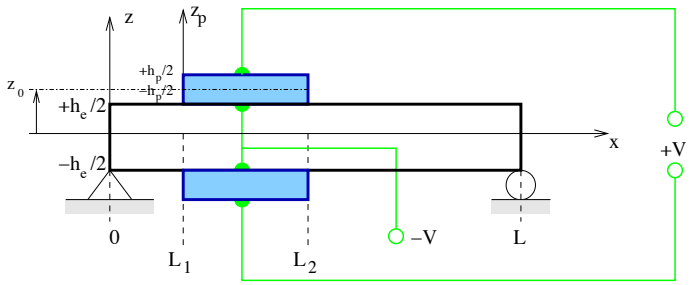

Fig. 2. Elastic plate sandwiched between two identical piezoelectric elements.

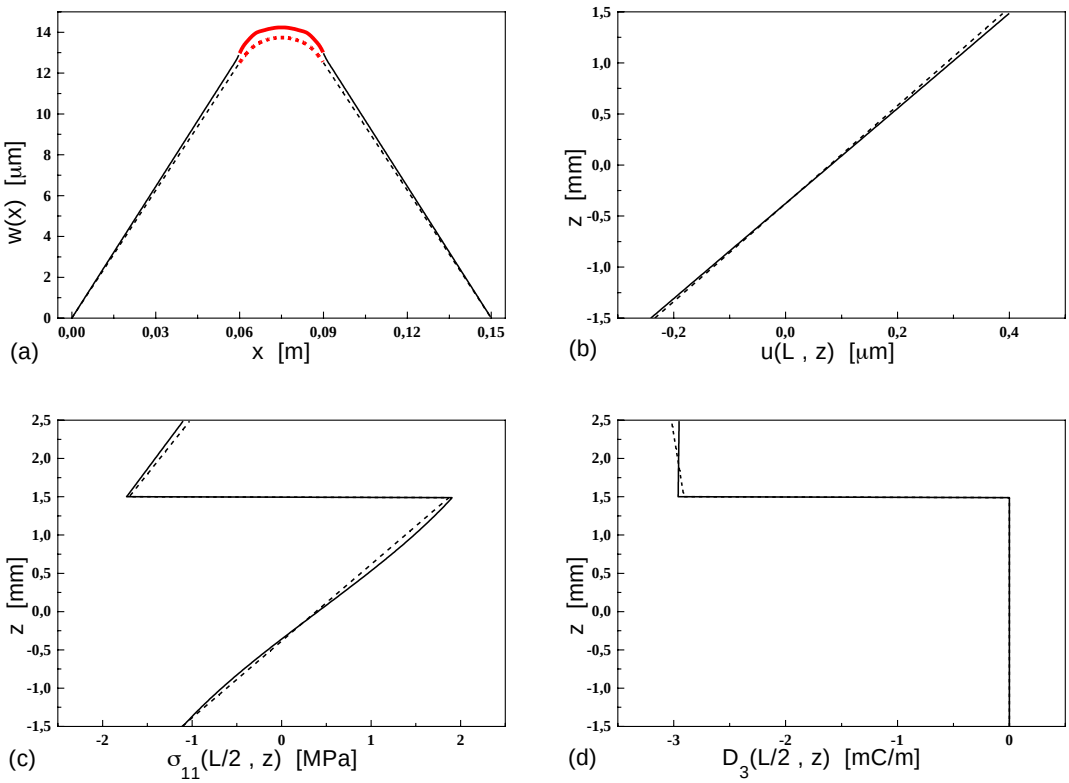

Fig. 3. Numerical results for the bilayer configuration (patch located at x=$L/2$) for an applied electric potential [Present model (solid-line) - Simplified model (dashed-line)].

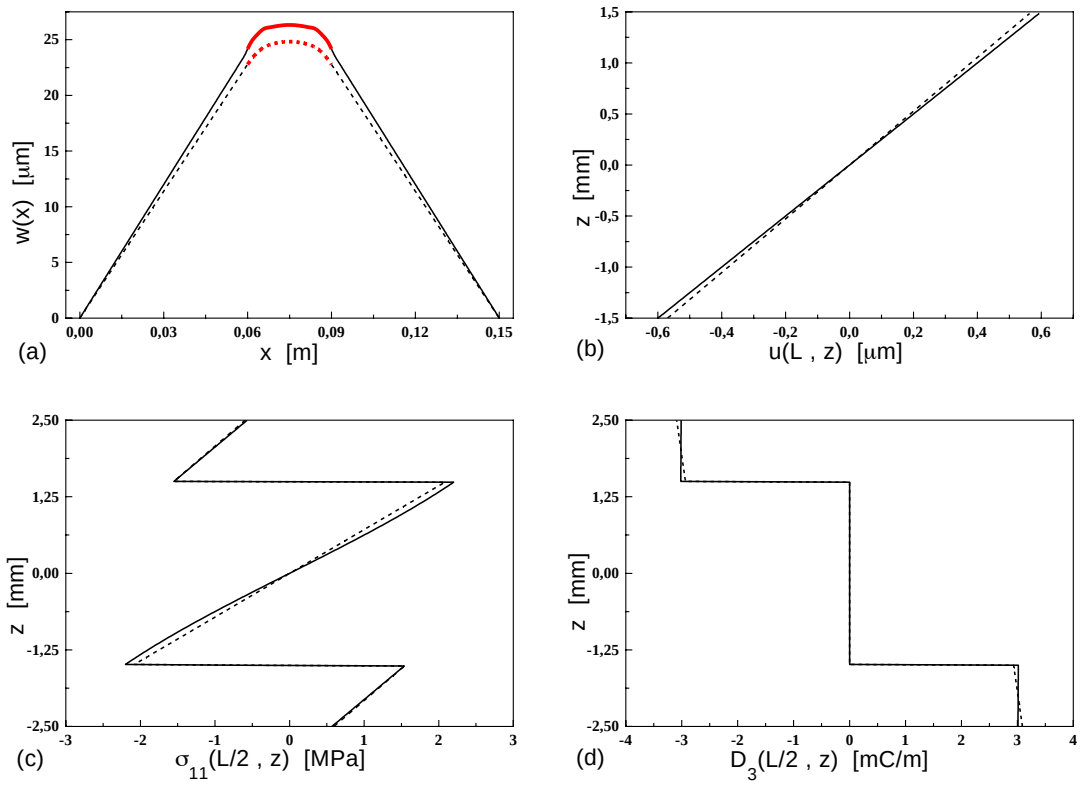

Fig. 4. Numerical results for the sandwich configuration (patch located at x=$L/2$) for an applied electric potential [Present model (solid-line) - Simplified model (dashed-line)].

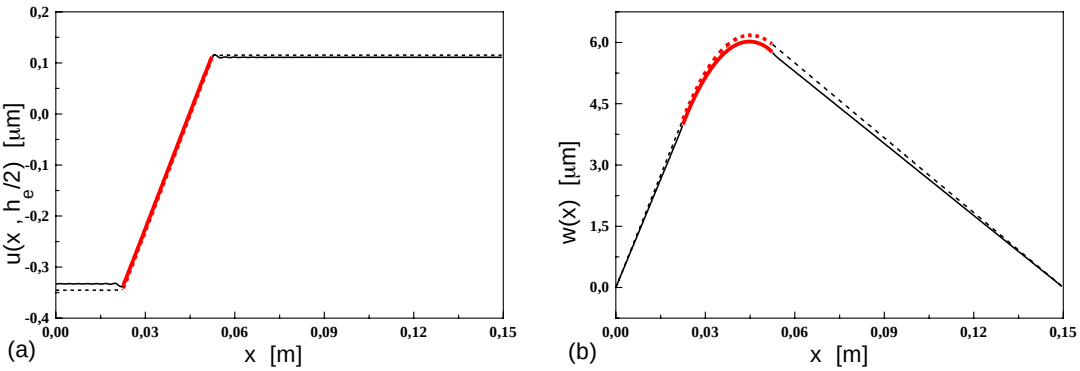

Fig. 5. Numerical results for the bilayer configuration (patch located at x=$L/4$) for an applied electric potential [Present model (solid-line) - Simplified model (dashed-line)].

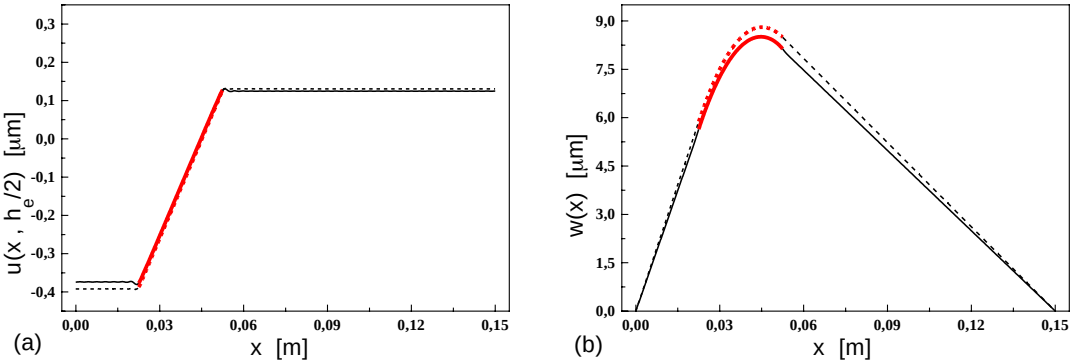

Fig. 6. Numerical results for the sandwich configuration (patch located at x=$L/4$) for an applied electric potential [Present model (solid-line) - Simplified model (dashed-line)].

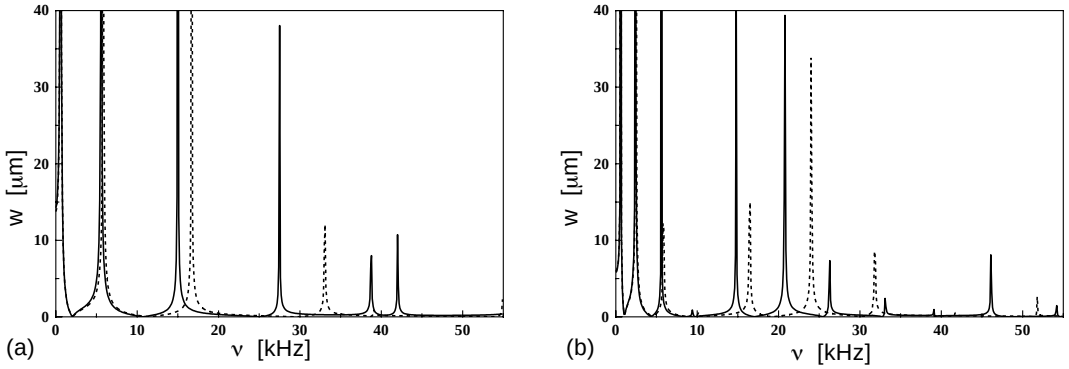

Fig. 7. Spectrum frequencies for the bilayer configuration (patch position at x=$L/2$ (a) and x=$L/4$ (b)) [Present model (solid-line) - Simplified model (dashed-line)].

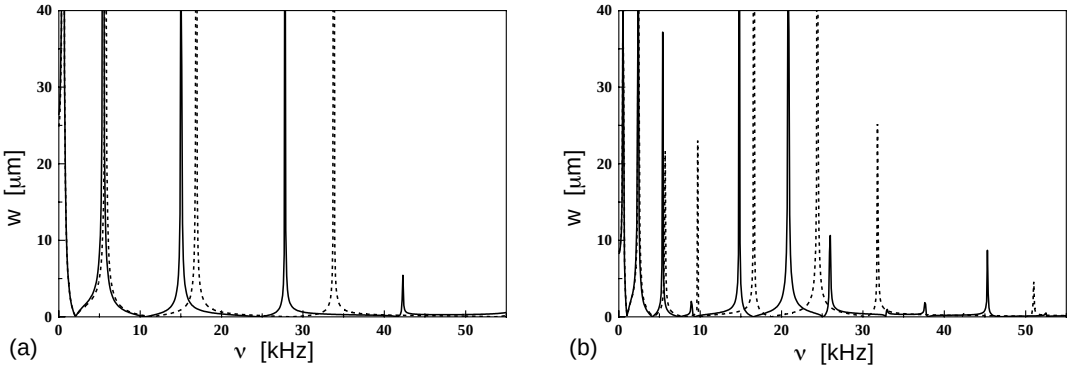

Fig. 8. Spectrum frequencies for the sandwich configuration (patch position at x=$L/2$ (a) and x=$L/4$ (b)) [Present model (solid-line) - Simplified model (dashed-line)].